El Cezeri
Journal of Science and Engineering
ISSN: 2148-3736

Research Article

Exploring the Influence of Various Solvents on the Structural, Optical, and Spectroscopic Properties of MgO

Bast Ahmed Mohammed[1a], Rebaz Obaid Kareem[2b*], Niyazi Bulut[3c], Tuna Demirci[4d], Erdem Elibol[4e], Filiz Ercan[6f], Ismail Ercan[5g], Tankut Ates[7h], Omer Kaygili[3i]

[1] Department of Applied Physics, College of Science, Charmo University, Chamchamal,Iraq
[2] Physics Department, College of Science, University of Halabja,46018, Halabja,Iraq
[3] Department of Physics, Faculty of Science, Firat University, Elazig,Türkiye
[4] Scientific and Technological Research Laboratory, Düzce University, Düzce,Türkiye
[5] Department of Electrical and Electronics Engineering, Faculty of Engineering, Düzce University, Türkiye
[6] College of Science, Basic and Applied Scientific Research Center, Nanomaterials Technology Unit, Imam Abdulrahman Bin Faisal University, Dammam, Saudi Arabia
[7] Department of Engineering Basic Sciences, Faculty of Engineering and Natural Sciences, Malatya Turgut Özal University, Battalgazi, Malatya, Türkiye

obedrebaz9@gmail.com

DOI : 10.31202/ecjse.1457824
Received: 24.03.2024 Accepted: 28.05.2024
How to cite this article:
Bast Ahmed Mohammed, Rebaz Obaid Kareem, Niyazi Bulut, Tuna Demirci, Erdem Elibol, Filiz Ercan, Ismail Ercan, Tankut Ates, Omer Kaygili, " Exploring the Influence of Various Solvents on the Structural, Optical, and Spectroscopic Properties of MgO", El-Cezeri Journal of Science and Engineering, Vol: 11, Iss: 3, (2024), pp.(283-287).
ORCID: [a]0009-0004-3774-633X; [b]0000-0001-6273-1309; [c]0000-0003-2863-7700; [d]0000-0001-8933-4944; [e]0000-0003-0328-5534; [f]0000-0002-3533-0726; [g]0000-0001-6490-3792; [h]0000-0002-4519-2953; [i]0000-0002-2321-1455.

Abstract : Magnesium oxide (MgO) samples were manufactured at different temperatures using various solvents of water and ethanol. MgO structure was also modeled and its vibration modes were calculated. The kind of solvent as-used in the synthesis and calcination temperature caused changes in the lattice parameter, crystallinity, and crystallite size. The crystallite size increased with increasing production temperature for both series of the MgO. The morphology and bandgap energy were also affected significantly by the solvent and calcination temperature.

Keywords : MgO, Bandgap energy.

1 Introduction

As an economical magnesium composite, magnesium oxide (MgO) is the primary and essential basic refractory mineral and can be employed in steel and iron commercial applications. MgO can be created through either natural or artificial processes. MgO can be found naturally as magnesium carbonate or artificially through the use of magnesium chloride derived from salts and seawater [1]. MgO is composed of Mg^{2+} and O^{2-} ions. In this substance, the d-orbital is unoccupied due to the chemical configuration of the ions [2]. MgO maintains a high degree of stability in both oxidizing and reducing atmospheres, withstanding temperatures of up to 2300°C and 1700°C, respectively [3]. Due to its low cost, resistance to corrosive environments, and a high melting point of 2800 °C, MgO is one of the essential substances [4]. MgO possesses a bandgap energy of 7.8 eV, making it a good insulator due to the absence of free electrons in its outer shell [2]. MgO is a type of ionic ceramic [5]. The molecular system of MgO consists of Mg and O atoms distributed along one-half of the diagonals of the cube [6], [7]. The main goal of the present study is to investigate the effects of the calcination temperature and the kind of solvent on the structural, morphological, and optical properties of MgO.

2 Materials and Methods

A cubic crystal structure of MgO illustrated in Figure 1a was designed using crystallography. Traditionally, experimental methods have been employed to study molecular structures, but due to their complexity and cost, computational approaches have gained popularity in recent years for their efficiency and ability to provide valuable insights. Our primary objective is to precisely optimize MgO's molecular structure and comprehend its electronic properties. MgO structure was investigated extensively using the B3LYP/6-31g method, and we extended our analysis to MgO's vibrational characteristics. Employing Fourier transform infrared (FTIR) calculations with the same basis set and method, we explore the material's vibrational modes and delve into the intricate interactions between magnesium and oxygen atoms. Eight solutions, each of 250mL of 0.4M magnesium nitrate hexahydrate (Merck), were prepared in different beakers using distilled water and ethanol (Sigma-Aldrich) as the solvents of the first and second groups. These solutions were stirred in a magnetic stirrer for 180 minutes without heating and then were put into an oven at 90°C for 48 hours. After drying, the as-obtained powders were heated in an electric furnace at 740, 840, 940,

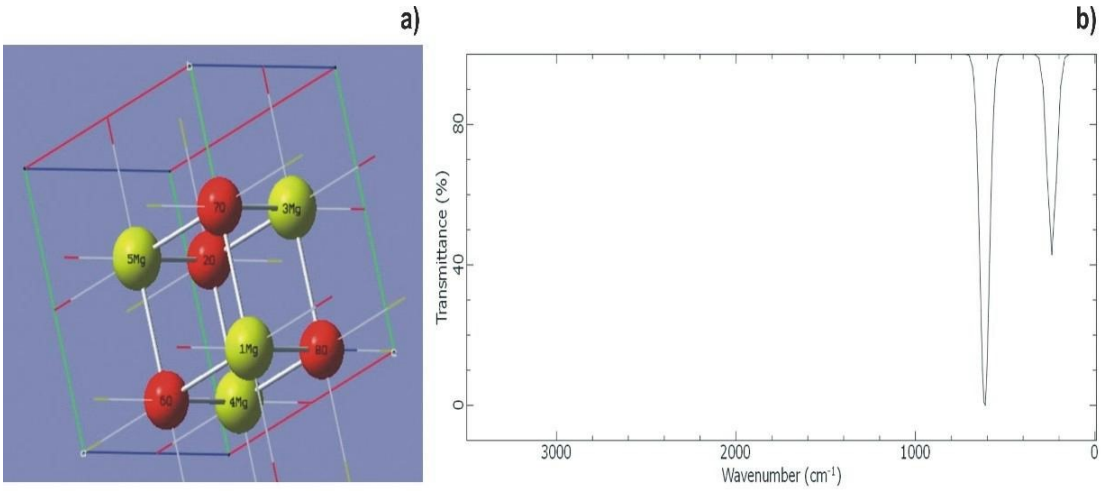

Figure 1: a) The cubic crystal structure (red and green colors represent O2- and Mg2+ ions), and b) FTIR spectrum of MgO

and 1040°C for 90 minutes for each group. According to the as-used solvent and heating temperature, the samples were named W740, W840, W940, and W1040 for the group prepared by distilled water, and the rest ones prepared by ethanol were referred to as E740, E840, E940, and E1040. A Rigaku Benchtop Miniflex diffractometer with CuK_{α} radiation was used to collect the XRD data. An FEI-Quanta FEG 250 scanning electron microscope was used for analyzing the morphology. A Spectro UV-Vis double-beam spectrophotometer UVD-3200 was used to investigate the optical properties.

3 Results and Discussion

In FTIR calculations, we simulated the absorption of infrared radiation by the MgO system, which results in the excitation of molecular vibrations. These vibrations arise from the harmonic motion of atoms around their equilibrium positions in the optimized structure. The interpretation of the FTIR peaks shown in Figure1b allows us to discern various molecular vibrations, such as stretching and bending modes of chemical bonds. By analyzing the intensities, frequencies, and shapes of these FTIR peaks, we can draw conclusions about the stability, symmetry, and electronic properties of the MgO system. Overall, the FTIR calculation represents a significant step towards a comprehensive characterization of MgO and paves the way for further investigations into its multifaceted properties.

In Figure 1b, we observe two prominent peaks that can be unequivocally linked to the stretching of the Mg-O bonds. These peaks are discernible as characteristic features in the graph, and their positions and intensities signify the specific vibrations associated with the Mg-O chemical bonds. Upon closer examination, the first peak, located at the lower wavenumber region, indicates the stretching vibrations of the Mg-O bonds. As the frequency increases along the x-axis, this peak exhibits its distinctive intensity, which arises from the collective movement of atoms within the MgO lattice. This stretching motion is a fundamental characteristic of the MgO molecular structure and can be identified through its unique spectral fingerprint. Likewise, the second peak, situated at the higher wavenumber range, also reflects the stretching of the MgO bonds. Although it appears at a different frequency compared to the first peak, it serves as another signature of the bonding behavior between Mg and O atoms in the material.

Figure 2a shows the XRD patterns of the as-produced MgOs and all the patterns are in a very good harmony with the standard data for MgO (JCPDS pdf no:87-0652) with the cubic crystal structure. These patterns indicate that all the samples have only a single phase of the MgO. The peaks belonging to the diffraction planes of (111), (200), and (220) are detected for all the samples. Some changes in the intensities and shifts in the positions of these peaks are seen. The lattice parameter (a), unit cell volume (V), crystallite size (t) and dislocation density (δ) of the MgOs were estimated using the following relations, respectively [8]:

$$a = d\sqrt{h^2 + k^2 + l^2} \tag{1}$$

$$V = a^3 \tag{2}$$

$$t = \frac{0.9\lambda}{\beta cos\theta} \tag{3}$$

$$\delta = \frac{1}{t^2} \tag{4}$$

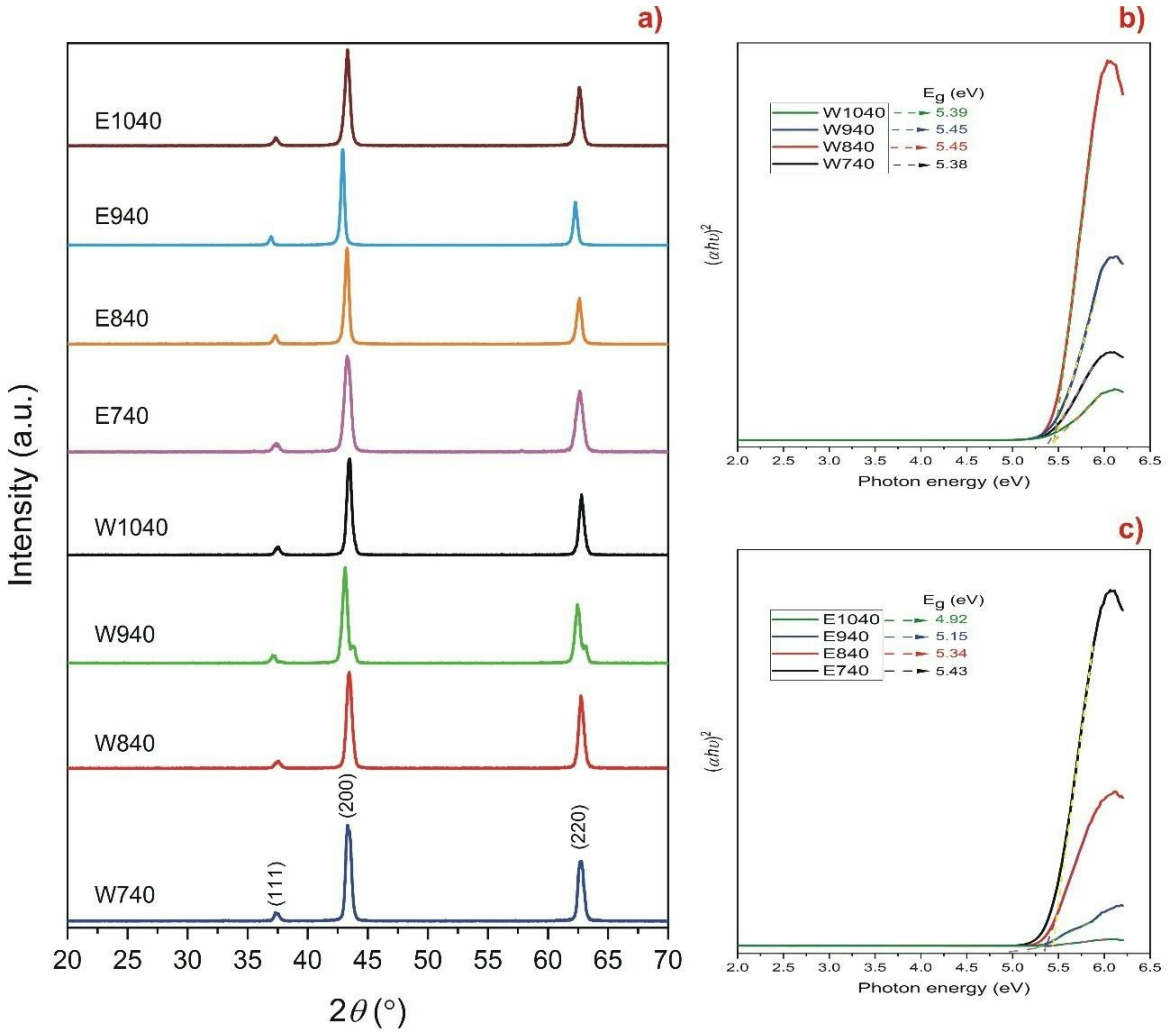

Figure 2: a) XRD patterns, and Tauc plots of the samples prepared with b) water and c) ethanol

Table 1: XRD analysis results.

Sample	a(nm)	$V(nm)^3$	t(nm)	$\delta(nm)^{-2}$	$X_C\%$
E740	0.4175	0.0728	19.21	0.0027	92.5
E840	0.4178	0.0729	25.55	0.0015	95.2
E940	0.4211	0.0747	36.14	0.0008	95.8
E1040	0.4174	0.0727	39.48	0.0006	94.1
W740	0.4184	0.0732	31.91	0.0010	93.8
W840	0.4172	0.0726	39.96	0.0006	93.7
W940	0.4126	0.0702	45.93	0.0005	93.6
W1040	0.4167	0.0724	59.37	0.0003	94.5

where d is the interplanar distance, β is the full width at half maximum and λ is the wavelength. Also, the crystallinity (XC) percent for each sample is listed in Table 1. The kind of solvent and calcination temperature are affected the lattice parameter and crystallite size. For two series, it is observed that the crystallite size increases with the calcination temperature. This finding is in a perfect agreement with the literature [8], [9]. For both series, the dislocation density decreases with the increasing production temperature and its small values indicate that the as-manufactured samples have high crystallinity [10]. High crystallinity values listed in Table 1 support this.

The optical bandgap energy (Eg) value for each sample was calculated using the following Tauc method [11]:

$$\alpha h\nu = A(h\nu - E_g)^n \tag{5}$$

where α is the absorption coefficient, $h\nu$ is the photon energy, A is a constant, and n is an exponent related to the type of electronic transitions ($n = 1/2$ for the directly allowed transition). The as-calculated values of the bandgaps and Tauc plots

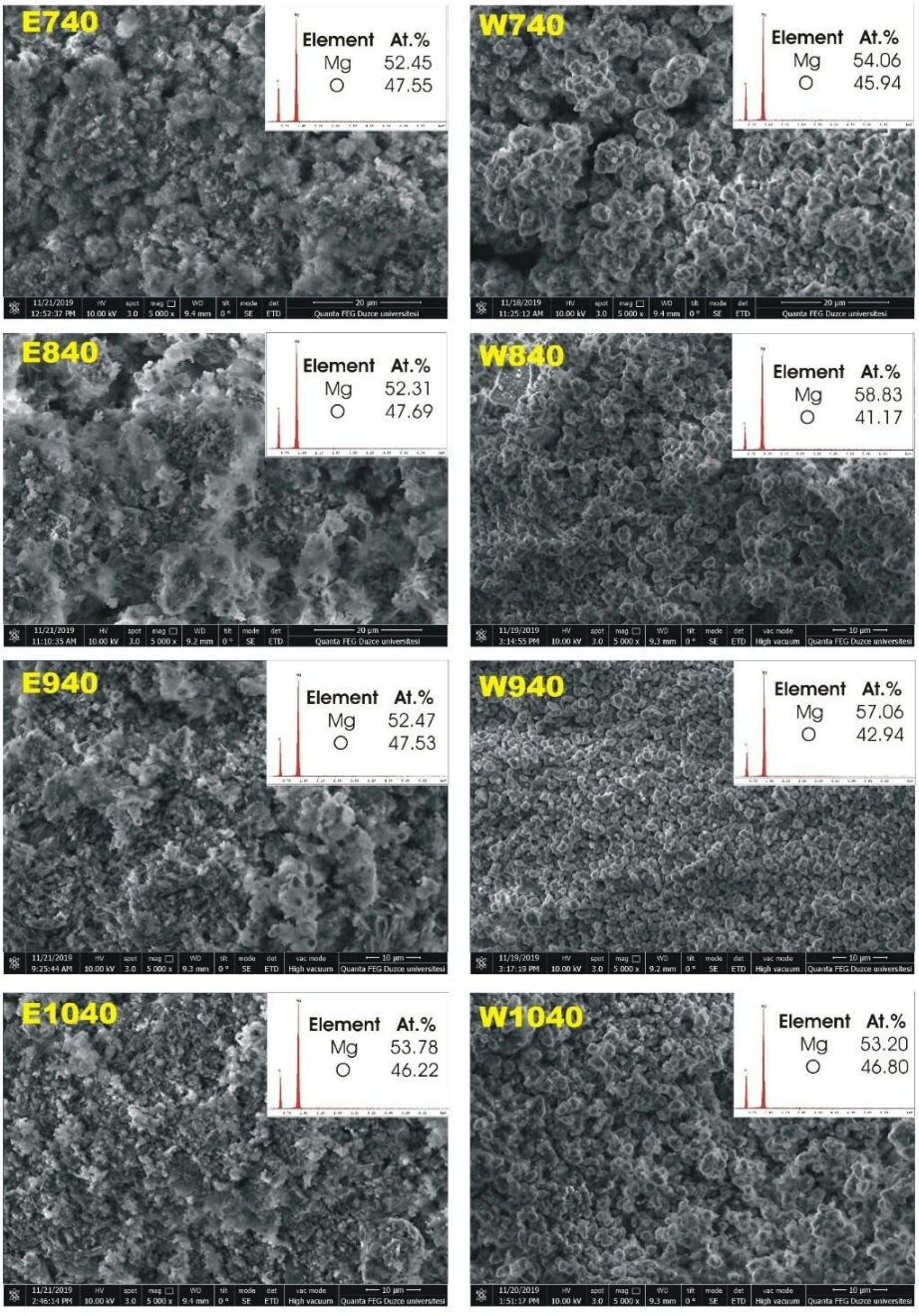

Figure 3: SEM and EDX analyses

of all the samples are shown in Figure 2b and Figure 2c. The Eg values are affected by both the solvent and manufacturing temperature.

For the samples of the E series, Eg decreases with increasing temperature. The as-calculated bandgap values are in the limits reported in the literature [12]–[14].

Figure 3 illustrates the morphological analysis for each sample. Both groups of MgO samples have fine-grained structures. Compared to the E group, the samples of the W group are composed of greater particles, which supports the XRD results. The EDX analyses confirm the MgO structure and verify that all the samples are composed of only Mg and O. The morphology is affected from the type of the solvent and calcination temperature.

4 Conclusion

The MgOs were prepared at different temperatures from 740 to 1040°C with a temperature step of 100°C for the solvents of ethanol and distilled water. It was observed that the crystallite size increased with the increase in the production temperature. The crystallinity, optical bandgap energy, morphology, and lattice parameter were affected by the type of solvent and calcination temperature.

Authorship contribution statement

B. Ahmad: R.O. Kareem: N. Bulut: Conceptualization, Writing-review & editing. T. Demirci: E. Elibol: F. Ercan: I. Ercan: T. Ates, O. Kaygili: Conceptualization, Methodology, Investigation

Declaration of competing interest

The authors declare that they have no known competing financial interests or personal relationships that could have appeared to influence the work reported in this paper.

References

[1] A. Jassim, S. Salmtori, and J. Jassam, ''Sustainable manufacturing process applied to produce magnesium oxide from sea water,'' in *IOP Conference Series: Materials Science and Engineering*, vol. 757, p. 012021, IOP Publishing, 2020.
[2] I. Ercan, O. Kaygili, T. Ates, B. Gunduz, N. Bulut, S. Koytepe, and I. Ozcan, ''The effects of urea content on the structural, thermal and morphological properties of mgo nanopowders,'' *Ceramics International*, vol. 44, no. 12, pp. 14523–14527, 2018.
[3] C. L. Wetteland, J. de Jesus Sanchez, C. A. Silken, N.-Y. T. Nguyen, O. Mahmood, and H. Liu, ''Dissociation of magnesium oxide and magnesium hydroxide nanoparticles in physiologically relevant fluids,'' *Journal of Nanoparticle Research*, vol. 20, pp. 1–17, 2018.
[4] D. Jesthi, A. Nayak, B. Routara, and R. Nayak, ''Evaluation of mechanical and tribological properties of glass/carbon fiber reinforced polymer hybrid composite,'' *International Journal of Engineering*, vol. 31, no. 7, pp. 1088–1094, 2018.
[5] R. Salomão, L. Bittencourt, and V. Pandolfelli, ''Aspects of magnesium oxide hydration in refractory castables compositions,'' *Ceramica*, vol. 52, pp. 146–150, 2006.
[6] W. G. Johnston and J. J. Gilman, ''Dislocation velocities, dislocation densities, and plastic flow in lithium fluoride crystals,'' *Journal of Applied Physics*, vol. 30, no. 2, pp. 129–144, 1959.
[7] J. Amodeo, S. Merkel, C. Tromas, P. Carrez, S. Korte-Kerzel, P. Cordier, and J. Chevalier, ''Dislocations and plastic deformation in mgo crystals: a review,'' *Crystals*, vol. 8, no. 6, p. 240, 2018.
[8] G. Monnet, ''Investigation of precipitation hardening by dislocation dynamics simulations,'' *Philosophical Magazine*, vol. 86, no. 36, pp. 5927–5941, 2006.
[9] L. Huang, Z. Yang, and S. Wang, ''Influence of calcination temperature on the structure and hydration of mgo,'' *Construction and Building Materials*, vol. 262, p. 120776, 2020.
[10] N. Pathak, S. K. Gupta, C. Prajapat, S. Sharma, P. Ghosh, B. Kanrar, P. K. Pujari, and R. Kadam, ''Defect induced ferromagnetism in mgo and its exceptional enhancement upon thermal annealing: a case of transformation of various defect states,'' *Physical Chemistry Chemical Physics*, vol. 19, no. 19, pp. 11975–11989, 2017.
[11] I. Sutapa, A. Wahid Wahab, P. Taba, and N. Nafie, ''Dislocation, crystallite size distribution and lattice strain of magnesium oxide nanoparticles,'' in *Journal of Physics: Conference Series*, vol. 979, p. 012021, IOP Publishing, 2018.
[12] J. Tauc, R. Grigorovici, and A. Vancu, ''Optical properties and electronic structure of amorphous germanium,'' *physica status solidi (b)*, vol. 15, no. 2, pp. 627–637, 1966.
[13] R. Sreekanth, J. Pattar, A. Anupama, and A. Mallikarjunaswamy, ''Synthesis of high surface area and plate-like magnesium oxide nanoparticles by ph-controlled precipitation method,'' *Applied Physics A*, vol. 127, pp. 1–9, 2021.
[14] S. Kiran, H. B. Albargi, G. Afzal, U. Aimun, M. N. Anjum, M. B. Qadir, Z. Khaliq, M. Jalalah, M. Irfan, and M. Abdullah, ''A zadirachta indica-assisted green synthesis of magnesium oxide nanoparticles for degradation of reactive red 195 dye: a sustainable environmental remedial approach,'' *Applied Water Science*, vol. 13, no. 10, p. 193, 2023.